Supporting Information

Helical Aromatic Oligoamide Macrocycle Incorporated with Ferrocene Unit for Encapsulation and Chirality Signalling of Zwitterionic Proline

Zejiang Liu,[∇,a] Maoxia Yang,[∇,a] Brice Kauffmann,[b] Juting Tan,[a] Yimin Cai,[a] Cheng Yang,*[,a] Xiaowei Li,*[,a] Wen Feng,[a] Ivan Huc[c] and Lihua Yuan*[,a]

[a] *College of Chemistry, Institute of Nuclear Science and Technology, Key Laboratory of Radiation Physics and Technology of Ministry of Education, Sichuan University, Chengdu 610064, Sichuan, China. Email: lhyuan@scu.edu.cn; lixw@scu.edu.cn; yangchengyc@scu.edu.cn*

[b] *Univ. Bordeaux, CNRS, INSERM, Institut Européen de Chimie Biologie (UMS3033/US001), 33600 Pessac, France*

[c] *Department of Pharmacy, Ludwig-Maximilians Universität München, D-81377 Munich, Germany*

[∇] These authors contributed equally to this work.

* Email: yangchengyc@scu.edu.cn; lixw@scu.edu.cn; lhyuan@scu.edu.cn

Table of Contents

1. General Methods

1-1. Materials

All chemicals were obtained from commercial suppliers and used as received unless otherwise noted. Reactions were conducted with oven-dried glassware under atmosphere or nitrogen and were stirred with Teflon-coated magnetic stir bars. Solvents were dried and distilled following standard protocols. Reaction processes were monitored by thin layer chromatography (TLC). All work-up and purification procedures were performed using reagent-grade solvents under ambient atmosphere. Column chromatography for compound purification was carried out using silica gel (100-200, and 300-400 mesh). Deuterated solvents for NMR experiments were purchased from Energy Chemical.

1-2. Instrumentation

Nuclear Magnetic Resonance (NMR): NMR spectra (^{1}H, ^{13}C, 2D experiments) were recorded using Bruker AVANCE AV II-400 or 600 MHz spectrometer at indicating temperature of 298 K. Chemical shifts are reported in δ values in ppm using tetramethylsilane (TMS) or residual solvent signals as the internal reference standards. Coupling constants (*J*) are denoted in Hz. Multiplicities are denoted as follows: s = singlet, d = doublet, t = triplet, dd = double doublet, m = multiples and br = broad. Structural assignments were made with additional information from gROESY experiment.

Ultraviolet–Visible (UV-vis) Spectroscopy Experiments: UV-vis spectra were recorded on a SHIMADZU UV-2600i spectrophotometer. HPLC grade solvents were used for all optical absorption experiments.

Single crystal X-ray data were measured on a Xcalibur E diffractometer with graphite monochromated Cu-Kα radiation (λ= 1.54184 Å). Data collection and structure refinement details can be found in the CIF files or obtained free of charge via https://www.ccdc.cam.ac.uk/.

High-resolution mass spectra: High-resolution mass spectra were recorded on a SCIEX X500R QTOF mass spectrometer operated in electrospray ionization mode.

The density functional calculations presented herein were completed with the B3LYP[1] functional in combination with the D3[2] dispersion correction as implemented in the

Gaussian 09 software[3]. The 6-311G(d)[4] basic from the Gaussian basis set library has been used in all the structural optimizations.

1-3. Procedure for the host–guest experiments

The host–guest experiments were carried out by mixing a chloroform solution of macrocycle **1** with a methanol solution of the amino acid, evaporating the solvents, and then redissolving the residue in chloroform-*d* or chloroform for measurement. For instance, 500 μL of a 10 mM chloroform solution of macrocycle **1** was combined with 150 μL of a 50 mM methanol solution of L-proline and mixed thoroughly. The solvents were removed under reduced pressure, after which 500 μL of $CDCl_3$ was added to afford an orange, homogeneous $CDCl_3$ solution containing 10 mM macrocycle **1** and 1.5 equivalents of L-proline.

1-4. Procedure for visualizing disorder of crystal Pro⊂1

By importing the crystal CIF file into the Mercury software, the various disorder models present in the structure can be visualized. The location of the nitrogen atom is assigned on the basis of relative strengths of the intermolecular hydrogen bonds arising from its occupation of alternative sites on the five-membered ring, in conjunction with the corresponding N–H bond lengths.

1-5. Single-Crystal Growth Methods

Single crystals of macrocycle **1** were obtained by slow vapor diffusion of diethyl ether into a 1,2-dichloroethane solution of **1** over 24 h.

Single crystals of the complex **Pro⊂1** were grown by slow diffusion of diethyl ether into a THF solution containing the host-guest complex with a 1:1 mole ratio over 48 h.

Single crystals of macrocycle **1-Me** adopting an inward amide N-H conformation were prepared by dissolving the compound in hot 1,2-dichloroethane, followed by slow vapor diffusion of diethyl ether into the solution over 12 h.

Single crystals of macrocycle **1-Me** with an outward amide NH conformation were obtained by dissolving the compound in hot 1,2-dichloroethane and carefully layering methanol over the solution. Crystals formed after 24 h via liquid–liquid diffusion.

2. Synthesis

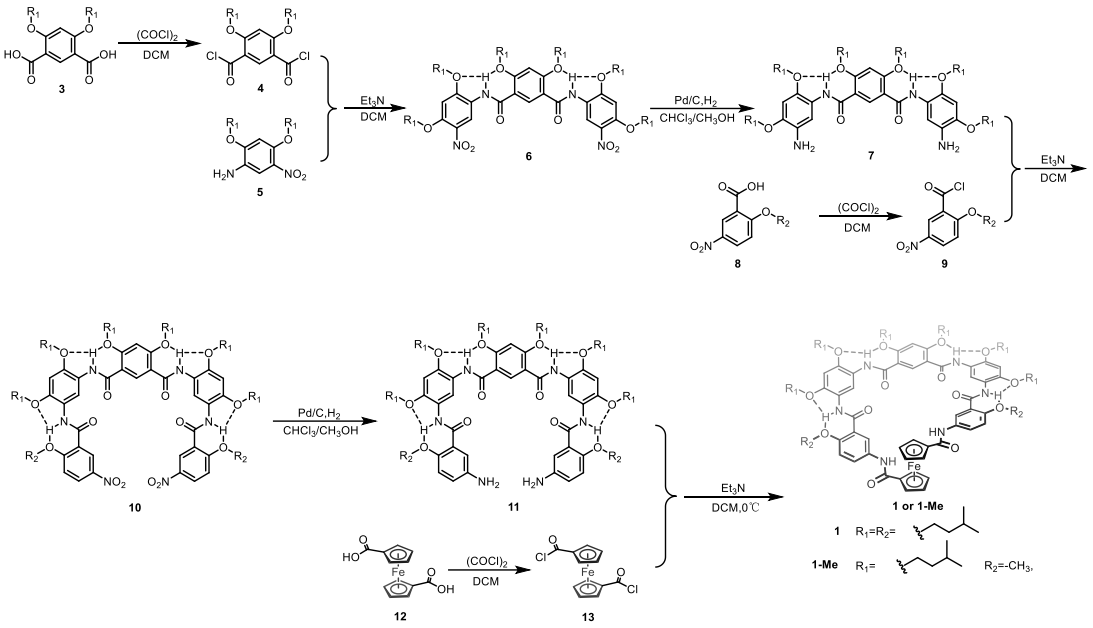

Scheme S1 Synthesis of macrocycles **1** and **1-Me**.

Compounds **6** and **10** were converted into compounds **7** and **11** by catalytic hydrogenation, respectively. Compounds **4**, **7**, **9**, **11** and **13** were used directly in the subsequent reaction without further purification. Compounds **3**, **4**, **5**, **8, 9, 12** and **13** were synthesized according to analogous literature procedures.[5]

Synthesis of compound 6: To a solution of compound **5** (1.01 g, 3.25 mmol) and Et_3N (1.27 g, 12.54 mmol) in dry CH_2Cl_2 (50 mL) was added compound **4** (0.45 g, 1.60 mmol). The reaction mixture was stirred at room temperature for 4 h. The solvent was removed under reduced pressure and the residue was redissolved in dry CH_2Cl_2 (40 mL). CH_3OH (80 mL) was added to induce precipitation. The solid was collected by filtration, washed with CH_3OH (3 × 60 mL), and dried under vacuum to give compound **6** as a light green–yellow powder (1.16 g, 85%).^{1}H NMR (400 MHz, $CDCl_3$) δ 9.60 (s, 2H), 9.17 (s, 2H), 8.87 (s, 1H), 6.46 (m, 3H), 4.29 (t, *J* = 7.2 Hz, 4H), 4.20 (t, *J* = 6.9 Hz, 4H), 4.04 (t, *J* = 6.6 Hz, 4H), 1.90-1.68 (m, 18H), 1.03-0.94 (m, 36H). ^{13}C NMR (101 MHz, $CDCl_3$) δ 161.8, 160.0, 152.8, 150.3, 137.2, 131.5, 121.4, 118.1, 114.5, 97.6, 96.4, 68.8, 68.5, 68.3, 37.7, 37.5, 37.4, 25.4, 25.2, 24.9, 22.8, 22.7, 22.5. HRMS (ESI) m/z: $[M + H]^+$ Calcd for $C_{50}H_{75}N_4O_{12}$ 923.5376; Found 923.5372.

General procedure for the synthesis of Compound 7 and 11: In the presence of H_2 gas, a mixture of compound **6** or **10** and a catalytic amount of Pd/C in $CHCl_3$/CH_3OH (80 mL, 7:1 v/v) was stirred at room temperature overnight. The solid catalyst was filtered off, and the resulting filtrate was concentrated under vacuum. The pure diamine **7** or **11** was obtained as a white solid. The reduced diamine was used directly for the subsequent coupling reaction.

Synthesis of Compound 10: To a solution of compound **7** (0.19 g, 0.22 mmol) and Et_3N (0.16 g, 1.07 mmol) in dry CH_2Cl_2 (50 mL) was added compound **9** (0.14 g, 0.50 mmol). The mixture was stirred at room temperature for 2 h. The reaction mixture was then concentrated under vacuum, and the residue was redissolved in dry CH_2Cl_2 (15 mL) and reprecipitated by the addition of CH_3OH (60 mL). The resulting solid was washed with methanol (3 × 60 mL), collected, and dried under vacuum to afford compound **10** as a yellow solid (0.23 g, 81%). ^{1}H NMR (400 MHz, $CDCl_3$) δ 9.54 (s, 2H), 9.48 (s, 2H), 9.18 (d, *J* = 3.0 Hz, 2H), 9.15 (s, 1H), 9.07 (s, 2H), 8.30 (dd, *J* = 9.2, 3.0 Hz, 2H), 7.11 (d, *J* = 9.2 Hz, 2H), 6.57 (m, 3H), 4.35 (t, *J* = 6.8 Hz, 4H), 4.27 (t, *J* = 6.6 Hz, 4H), 4.08 (t, *J* = 6.9 Hz, 8H), 1.90 – 1.71 (m, 24H), 1.01 – 0.93 (m, 48H). ^{13}C NMR (101 MHz, $CDCl_3$) δ 162.1, 161.1, 160.6, 160.0, 146.4, 146.0, 141.6, 137.8, 128.7, 127.8, 123.2, 121.1, 120.2, 117.7, 116.1, 113.0, 97.9, 97.0, 69.4, 68.5, 67.8, 38.0, 38.0, 37.6, 37.3, 25.2, 25.2, 25.2, 25.1, 22.7, 22.7, 22.6. HRMS (ESI) m/z: $[M + H]^+$ Calcd for $C_{74}H_{105}N_6O_{16}$ 1333.7582; Found 1333.7578.

Synthesis of Compound 10-Me: Compound **10-Me** was prepared following the procedure described for compound **10** and was obtained as a yellow block solid (88%). ^{1}H NMR (400 MHz, $CDCl_3$) δ 9.77 (s, 2H), 9.54 (s, 2H), 9.32 (s, 2H), 9.27 (s, 1H), 9.17 (d, *J* = 3.0 Hz, 2H), 8.07 (dd, *J* = 9.2, 3.0 Hz, 2H), 7.15 (d, *J* = 9.2 Hz, 2H), 6.60 (s, 1H), 6.47 (s, 2H), 4.30 (d, *J* = 6.8 Hz, 4H), 4.25 (s, 6H), 4.09 (t, *J* = 6.9 Hz, 4H), 4.01 (t, *J* = 6.8 Hz, 4H), 1.89 – 1.72 (m, 18H), 1.01 – 0.97 (m, 36H). HRMS (ESI) m/z: $[M + H]^+$ Calcd for $C_{66}H_{89}N_6O_{16}$ 1221.6330; Found 1221.6326.

Synthesis of macrocycle 1: A solution of compound **13** (0.04 g, 0.13 mmol) in dry CH_2Cl_2 (60 mL) was treated dropwise with a solution of compound **11** (0.14 g, 0.11 mmol) and Et_3N (0.10 g, 0.99 mmol) in dry CH_2Cl_2 (150 mL) under an argon atmosphere. After 2 h, the reaction mixture was concentrated under reduced pressure, and CH_3OH (60 mL) was added to precipitate the solid as the crude product. The crude product was further

purified by chromatography on silica gel (DCM/MeOH, 30:1, v/v) to afford product **1** as an orange solid (0.06 g, 35%). Note: Due to the thermal instability of macrocycle **1**, its melting point could not be determined. The compound undergoes thermal decomposition at approximately 260 °C prior to melting.^{1}H NMR (400 MHz, $CDCl_3$) δ 10.03 (s, 2H), 9.74 (s, 2H), 9.45 (s, 2H), 9.42 (s, 1H), 8.50 (dd, *J* = 9.0, 2.9 Hz, 2H), 8.17 (d, *J* = 2.9 Hz, 2H), 7.77 (s, 2H), 7.03 (d, *J* = 9.0 Hz, 2H), 6.56 – 6.54 (m, 3H), 4.99 (m, 4H), 4.49 (m, 4H), 4.32 – 4.26 (m, 8H), 4.14 – 4.10 (m, 8H), 1.94 – 1.71 (m, 24H), 1.08 – 0.91 (m, 48H). ^{13}C NMR (101 MHz, $CDCl_3$) δ 167.7, 159.5, 152.7, 145.0, 144.9, 132.6, 123.7, 123.3, 121.6, 121.4, 116.9, 113.5, 98.1, 68.6, 68.4, 67.9, 38.1, 38.0, 37.6, 37.6, 25.3, 25.3, 25.2, 25.1, 22.7, 22.7. HRMS (ESI) m/z: $[M + H]^+$ Calcd for $C_{86}H_{115}FeN_6O_{14}$ 1511.7815; Found 1511.7812.

Synthesis of macrocycle 1-Me: To a solution of compound **13** (0.05 g, 0.16 mmol) in dry CH_2Cl_2 (60 mL) under an argon atmosphere was added dropwise a solution of compound **11-Me** (0.15 g, 0.13 mmol) and Et_3N (0.09 g, 0.89 mmol) in dry CH_2Cl_2 (150 mL). The mixture was stirred at room temperature, during which an orange block-crystalline precipitate of compound **1-Me** gradually formed. The solid was collected by filtration, rinsed with CH_2Cl_2 (3 × 40 mL), and dried in vacuo to give compound **1-Me** as an orange solid (0.08 g, 44%). Note: Due to the thermal instability of macrocycle **1-Me**, its melting point could not be determined. The compound undergoes thermal decomposition at approximately 260 °C prior to melting. ^{1}H NMR (400 MHz, $CDCl_3$) δ 10.18 (s, 2H), 9.74 (s, 2H), 9.44 (m, 3H), 8.57 (m, 2H), 8.23 (m, 2H), 7.04 (d, *J* = 9.0 Hz, 2H), 6.55 (m, 3H), 5.06 (m, 4H), 4.48 (m, 4H), 4.36 – 4.01 (m, 18H), 2.01 – 1.74 (m, 18H), 1.29 – 1.26 (m, , 12H), 1.04 – 0.99 (m , 24H). HRMS (ESI) m/z: $[M + H]^+$ Calcd for $C_{78}H_{99}FeN_6O_{14}$ 1399.6563; Found 1399.6561.

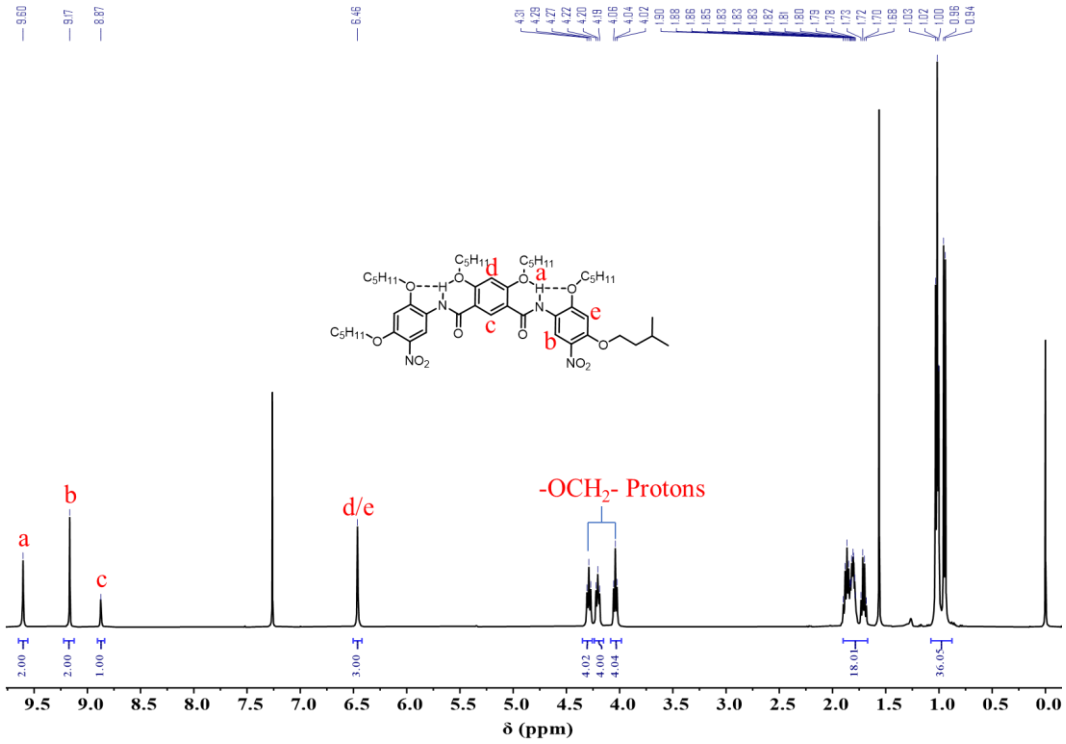

Figure S1 ^{1}H NMR spectrum (400 MHz, $CDCl_3$, 298 K) of compound **6**.

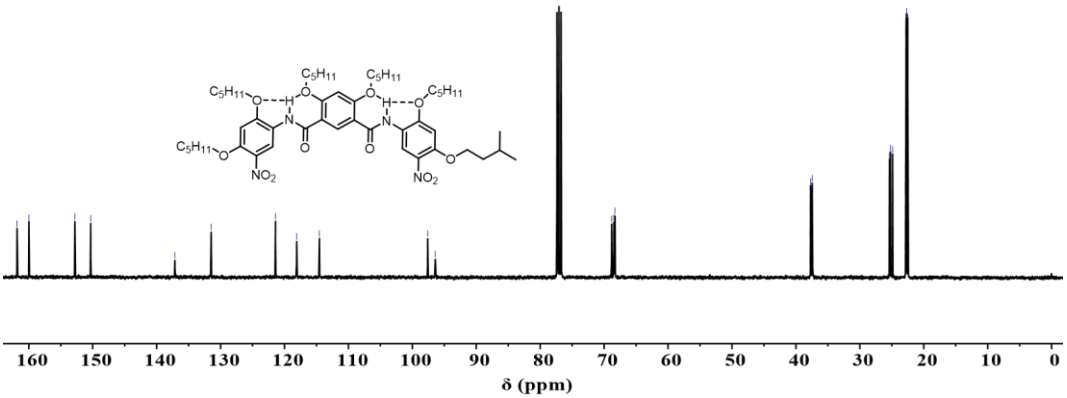

Figure S2 ^{13}C NMR spectrum (101 MHz, $CDCl_3$, 298 K) of compound **6**.

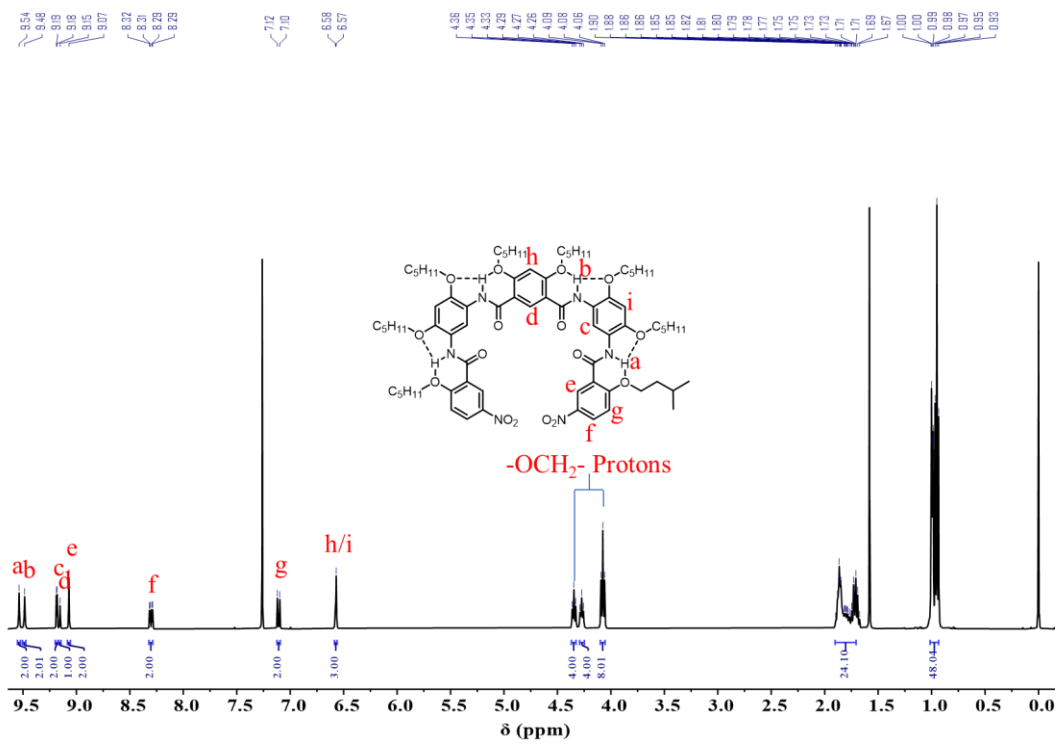

Figure S3 ^{1}H NMR spectrum (400 MHz, $CDCl_3$, 298 K) of compound **10**.

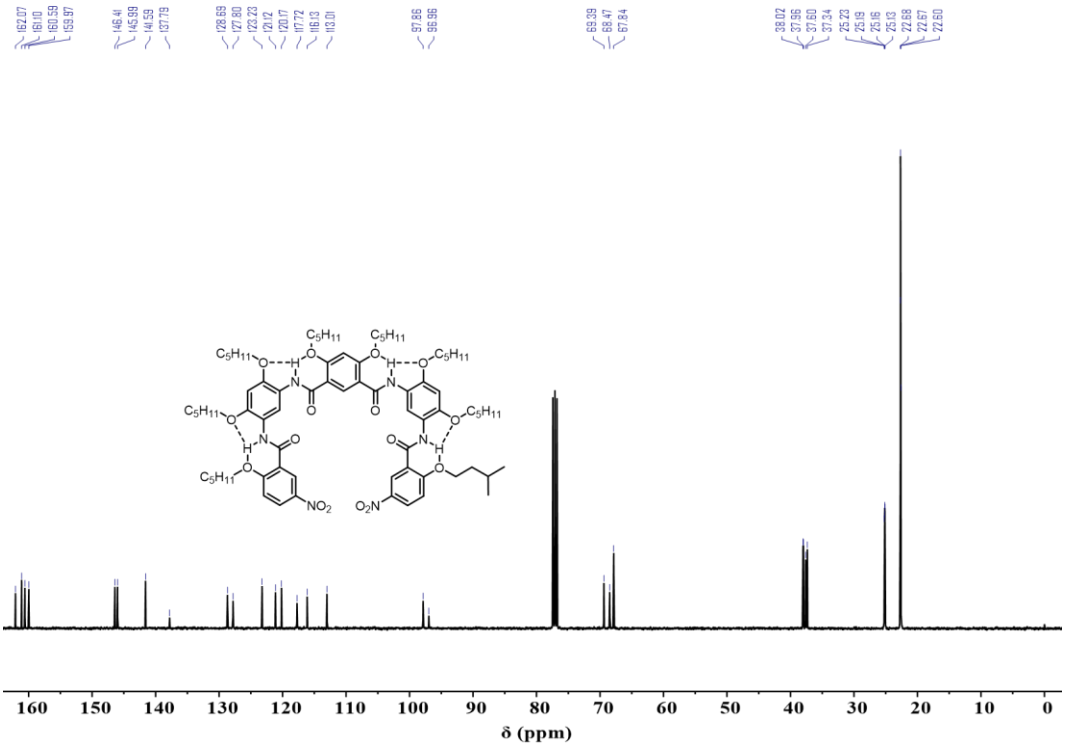

Figure S4 ^{13}C NMR spectrum (101 MHz, $CDCl_3$, 298 K) of compound **10**.

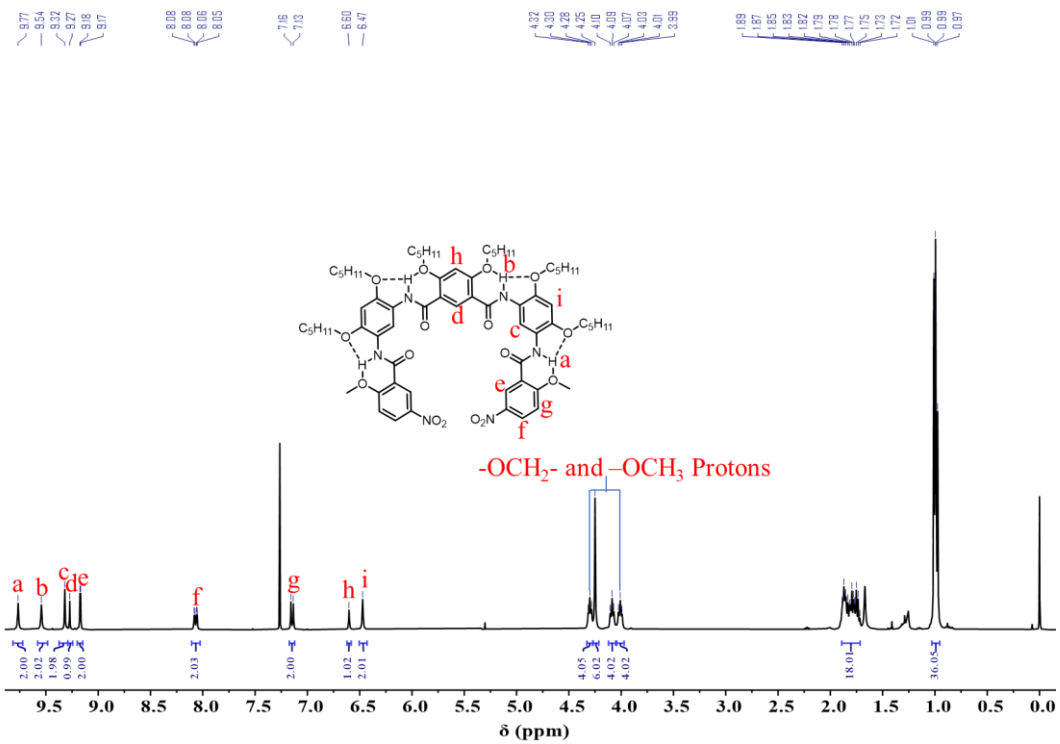

Figure S5 ^{1}H NMR spectrum (400 MHz, $CDCl_3$, 298 K) of compound **10-Me**.

Due to its rapid precipitation from the hot solution, compound **10-Me** could not be characterized by ^{13}C NMR spectroscopy.

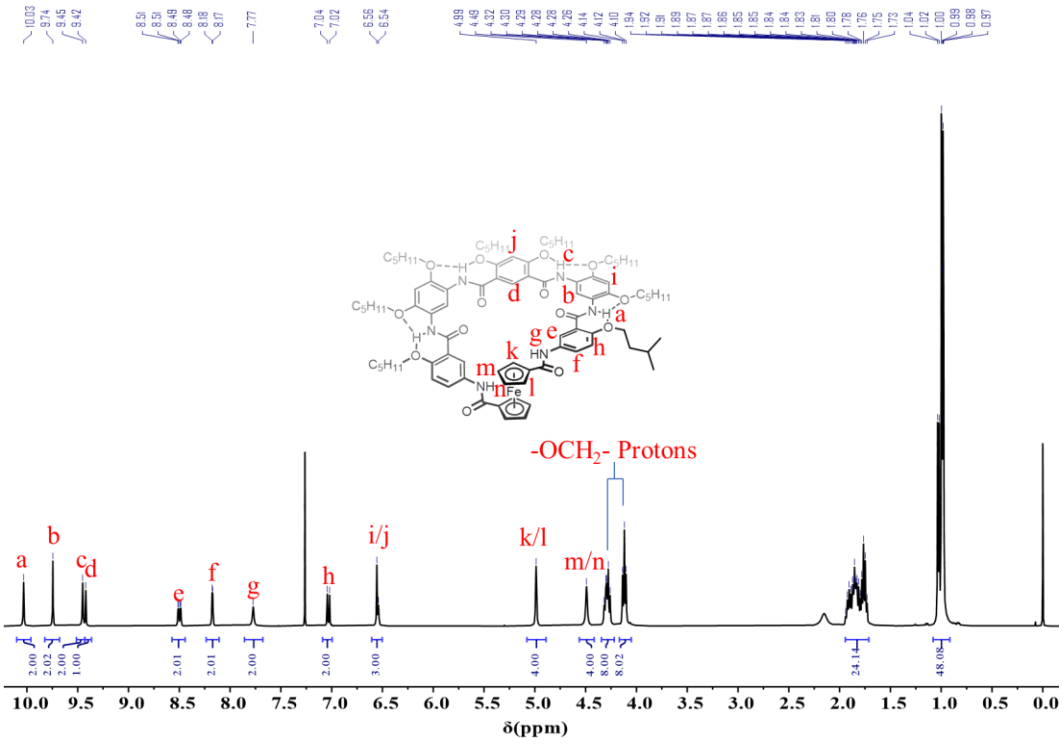

Figure S6 ^{1}H NMR spectrum (400 MHz, $CDCl_3$, 298 K) of compound **1**.

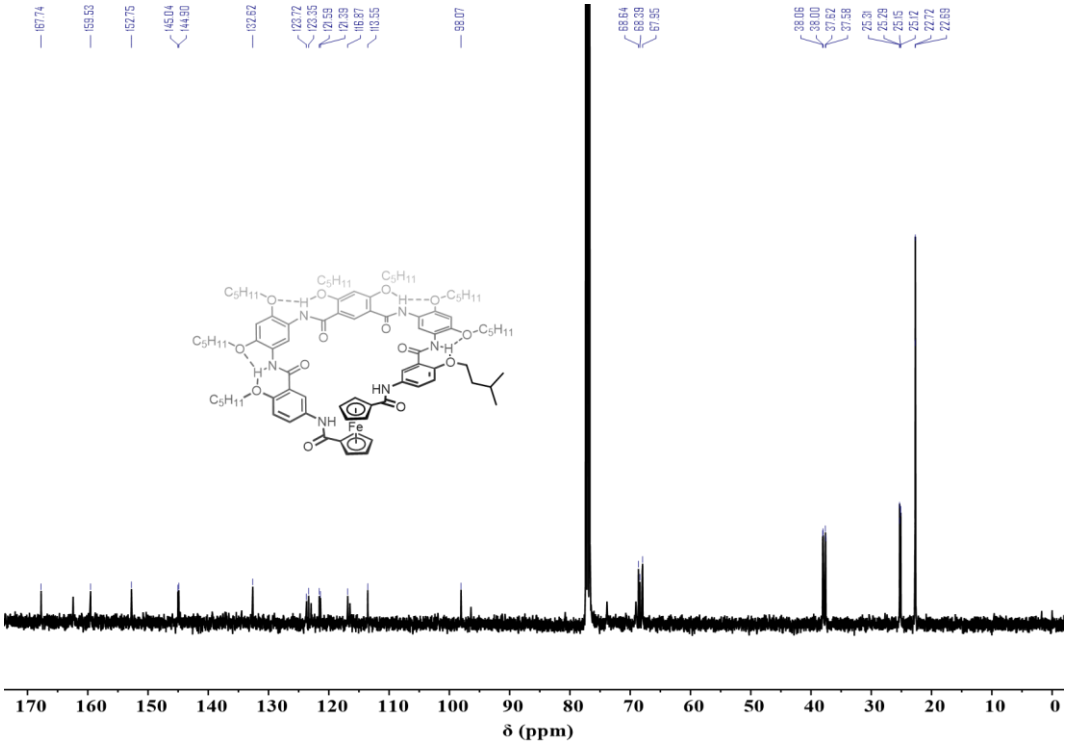

Figure S7 ^{13}C NMR spectrum (101 MHz, $CDCl_3$, 298 K) of compound **1**.

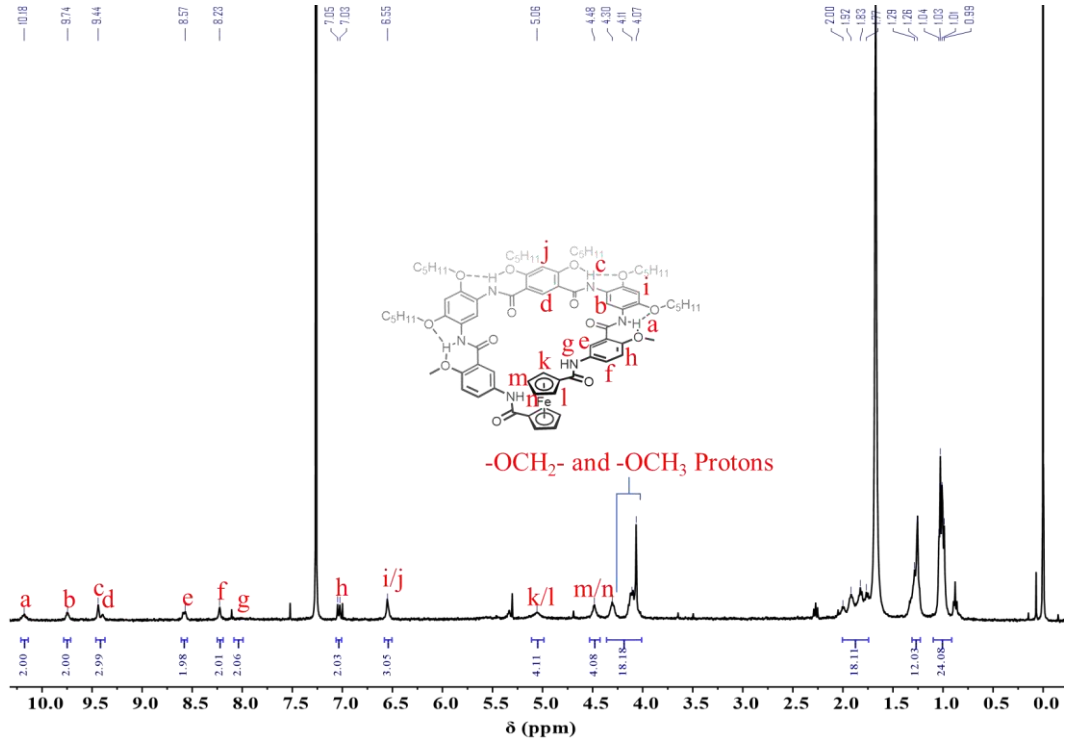

Figure S8 ^{1}H NMR spectrum (400 MHz, $CDCl_3$, 298 K) of compound **1-Me**.

Due to its limited solubility in all but hot $ClCH_2CH_2Cl$, compound **1-Me** could not be characterized by ^{13}C NMR spectroscopy.

3. 2D-ROESY ^{1}H NMR spectra of macrocycle 1

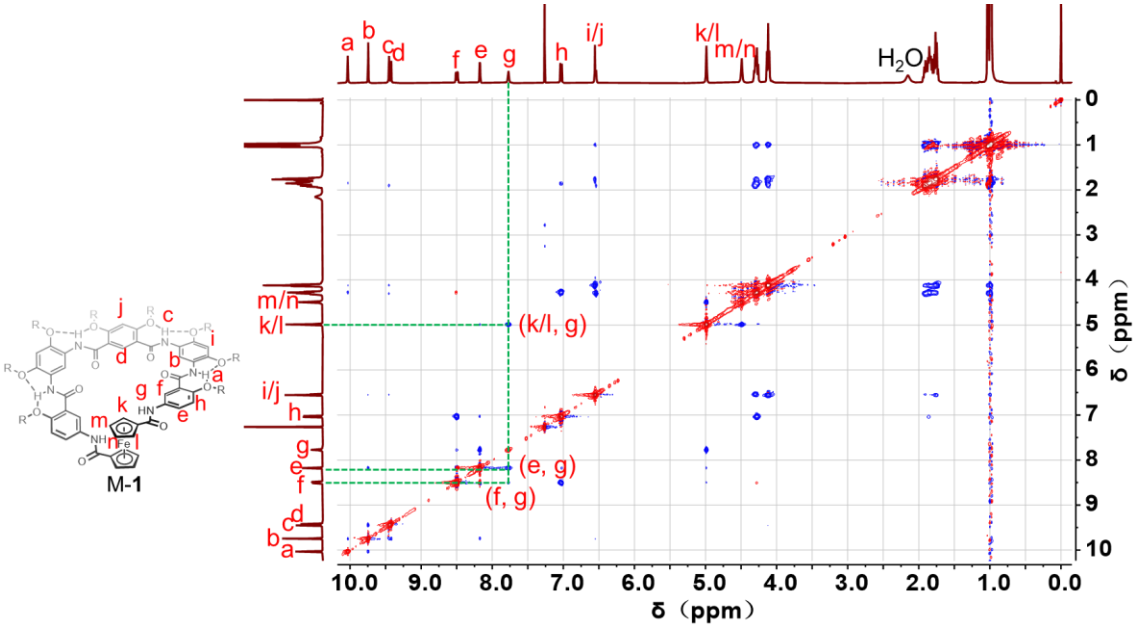

Figure S9 2D ROESY NMR of spectrum of macrocycle **1** (400 MHz, 10.0 mM, 298 K, $CDCl_3$).

4. Concentration dependent ^{1}H NMR spectra of macrocycle 1

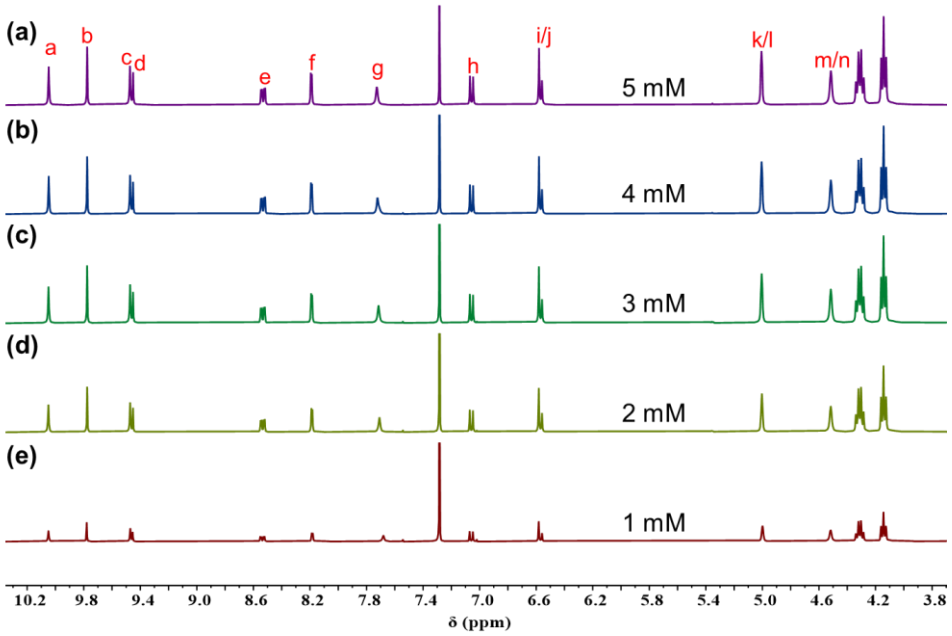

Figure S10 Stacked partial ^{1}H NMR spectra (400 MHz, $CDCl_3$, 298 K) of **1** at indicating concentrations of macrocycle **1** (a) 5.0 mM, (b) 4.0 mM, (c) 3.0 mM, (d) 2.0 mM and (e) 1.0 mM.

5. DFT calculations for the macrocycle and its binding mode towards amino acid

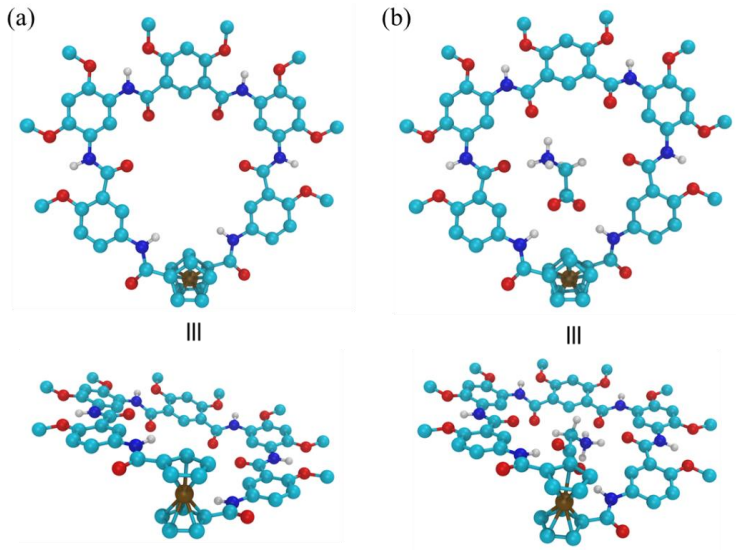

Figure S11 Optimized structures of (a) macrocycle **1** and (b) complex glycine⊂**1** obtained by D3-B3LYP/6-311G(d) method. Top views (top) and front views (bottom) are shown. For clarity, side chain and CH protons of macrocycle are omitted.

6. Transformation Barrier Between the *P* and *M* Conformations of Macrocycle 1

Protons	Coalescence temperature (K)	Δδ(ppm)	Δν (Hz)	k_c (S^{-1})	ΔG‡ (kcal/mol)
k, l	243	0.23	138	307.3	11.4
m, n	253	0.37	222	494.4	11.6

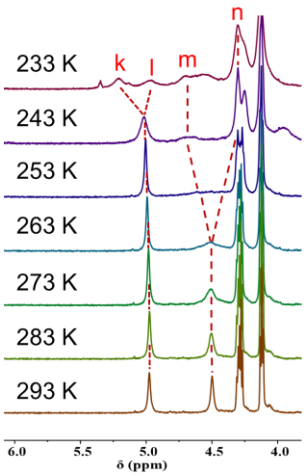

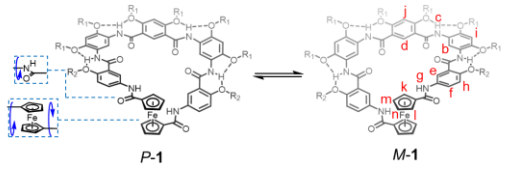

$\Delta\nu = \Delta\delta \times 600$ MHz $k_c = \pi(\Delta\nu)/\sqrt{2}$

k_c is the rate of enantiomerization at the coalescence temperature

The approximate barrier of this transformation ΔG‡ can be calculated according to the Eyring equation:

$$k_c = \frac{k_B T_c}{h} e^{-\Delta G^{\ddagger}/RT_c}$$

$k_B = 1.381 \times 10^{-23}$ J/K $h = 6.626 \times 10^{-34}$ J·sec

$R = 8.314$ J/(mol·K) T_c is coalescence temperature

Figure S12 Calculation of the free energy barrier (ΔG‡) for the *P* and *M* interconversion based on the variable-temperature (VT) ^{1}H NMR data for macrocycle **1**. Using the coalescence temperature (T_c) of the split ferrocene proton resonances (assigned as *k*/*l* and *m*/*n* in **Figure S12**), the free energy of activation (ΔG‡) for the *P* and *M* interconversion was calculated to be approximately 11.5 kcal·mol^{-1}.

7. HRESI-MS and Job plot experiment for complex Pro⊂1

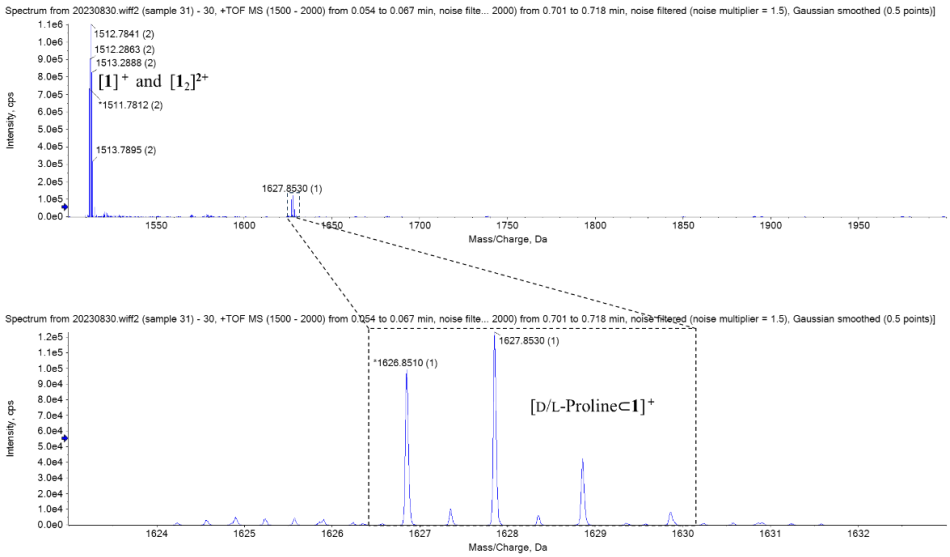

Figure S13 The HRESI-MS spectrum of an equimolar solution of macrocycle **1** and proline in $CHCl_3$ in the positive ion mode.

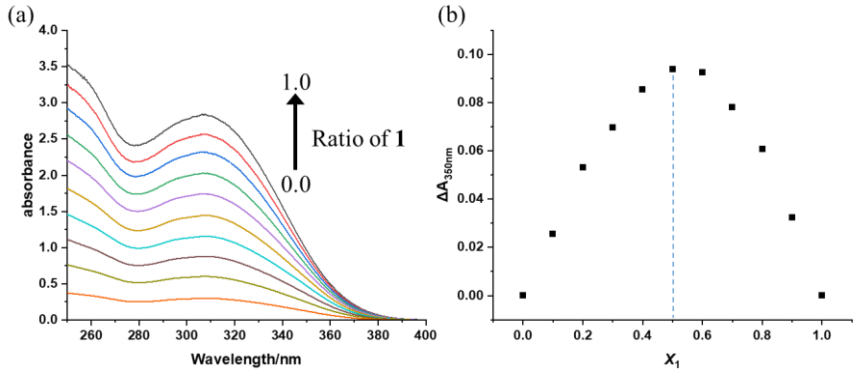

Figure S14 (a) Stacked plots of UV spectra of macrocycle **1** with D/L-Proline at a total concentration of 50 μM in $CHCl_3$, (b) Job plots between macrocycle **1** and D/L-Proline were obtained by plotting the changes of absorbance at 350 nm indicating a 1:1 stoichiometry.

8. Host guest complexation between macrocycle 1 and natural amino acids

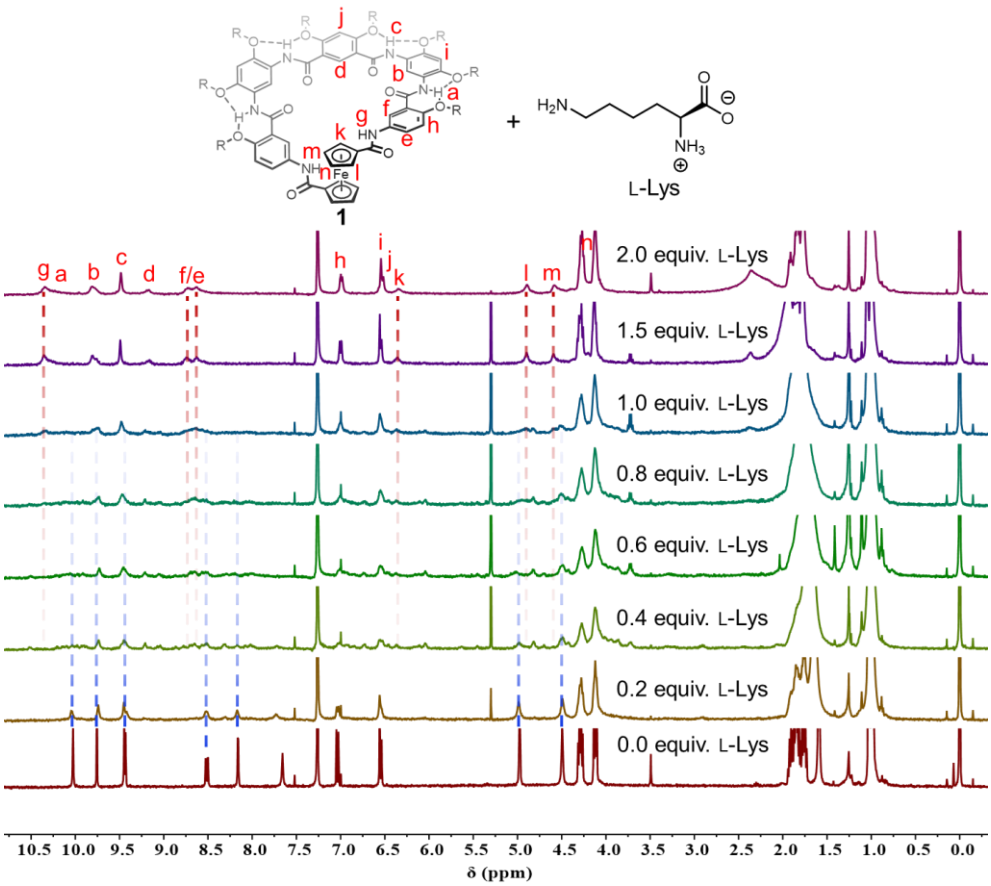

Figure S15 Stacked ^{1}H NMR spectra of macrocycle **1** (1.0 mM) upon addition of different equiv. of L-lysine (0–2.0 equiv.) in $CDCl_3$ (400 MHz, 298 K).

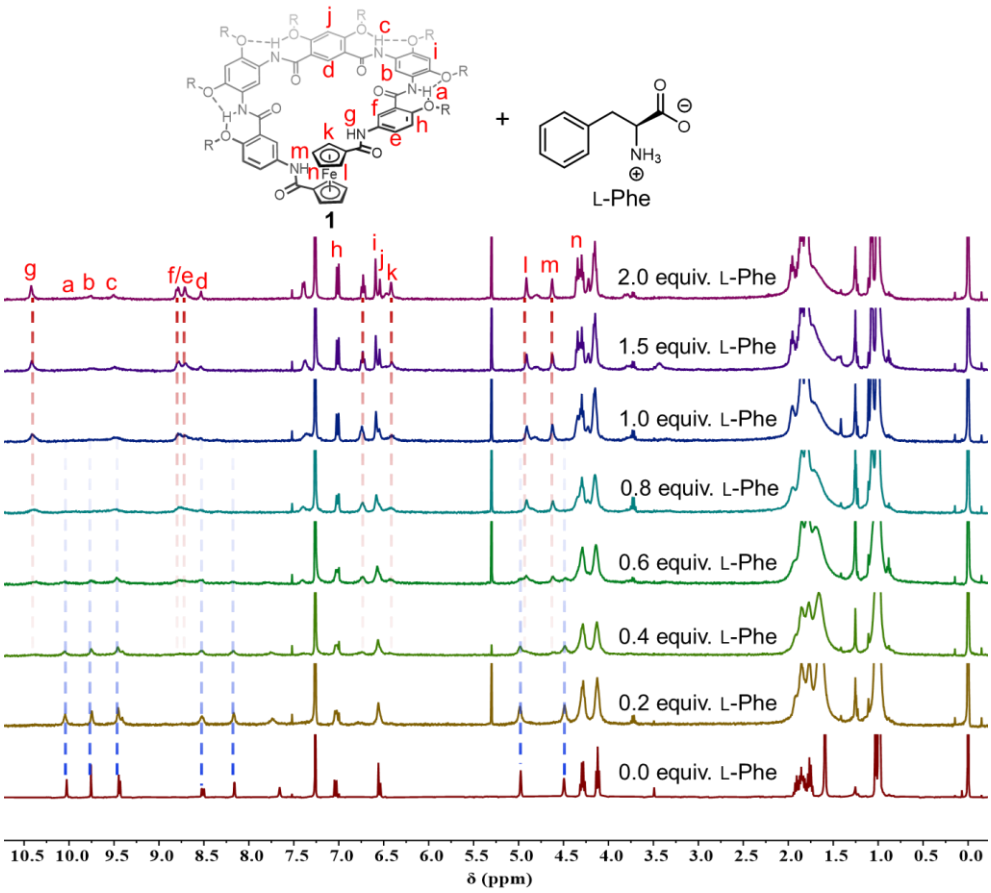

Figure S16 Stacked ^{1}H NMR spectra of macrocycle **1** (1.0 mM) upon addition of different equiv. of L-phenylalanine (0–2.0 equiv.) in $CDCl_3$ (400 MHz, 298 K).

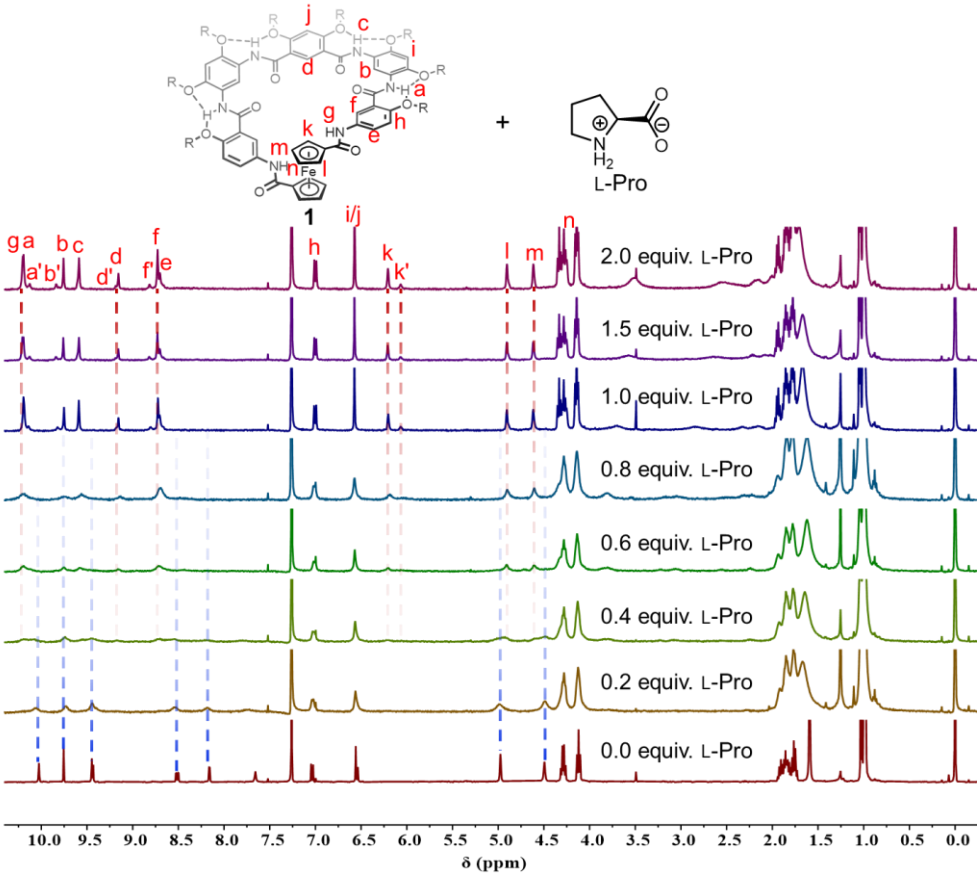

Figure S17 Stacked ^{1}H NMR spectra of macrocycle **1** (1.0 mM) upon addition of different equiv. of L-proline (0–2.0 equiv.) in $CDCl_3$ (400 MHz, 298 K).

Competitive NMR titration experiments

The competitive NMR titration experiments were carried out according to literature procedures.[6] In the NMR titration experiments, the amount of proline was gradually increased in a solution containing **1** (2.0 mM) and TBAB (400 mM), resulting in the signals of protons *b*, *c*, *e*, *f* and *g* of macrocycle **1** shifting in the ^{1}H NMR spectra. These chemical-shift changes arise from the formation of the complex L-Pro⊂**1**, which is more stable than the Br^-⊂**1** complex.

$$Br^- + [Br^- \subset \mathbf{1}] + \text{L-Pro} \longrightarrow Br^- + [\text{L-Pro} \subset \mathbf{1}]$$

Because the concentration of free bromide ion, [Br^-], remains effectively constant throughout the titration due to its large excess, the titration data can be fitted to a 1:1 binding isotherm to obtain the relative binding constant K_{rel}. Here, K_{Br^-} represents the binding constant between macrocycle **1** and TBAB, whereas $K_{\text{L-Pro}}$ represents the binding constant between macrocycle **1** and proline.

$$K_{rel} = \frac{[\text{L-Pro} \subset \mathbf{1}]}{[Br^- \subset \mathbf{1}] \times [Br^-]} = \frac{K_{\text{L-Pro}}}{K_{Br^-} \times [Br^-]} \qquad K_{\text{L-Pro}} = K_{rel} \times K_{Br^-} \times [Br^-]$$

NMR titration experiments for TBAB

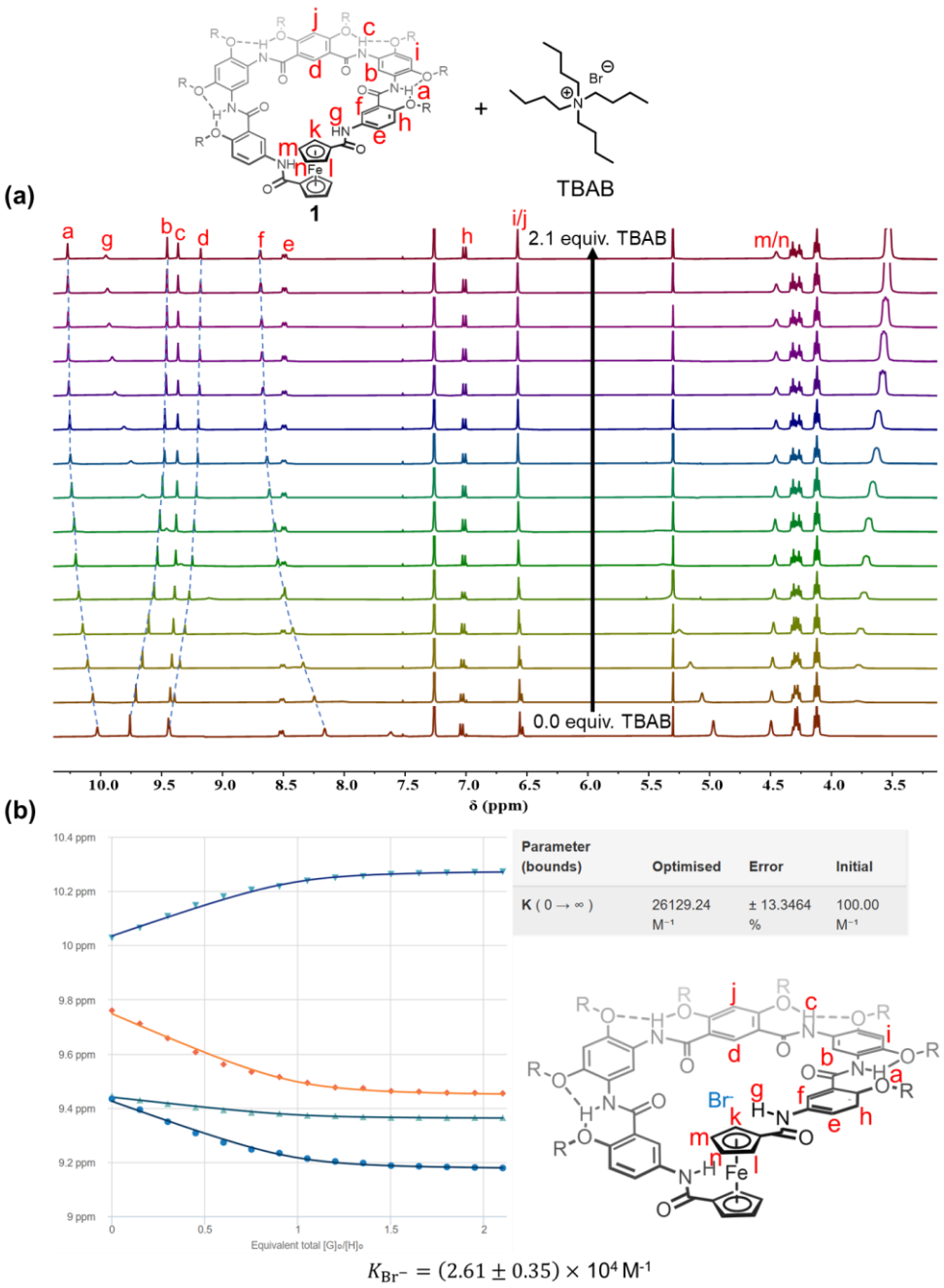

Figure S18 (a) Stacked plots of ^{1}H NMR spectra of macrocycle **1** (2.0 mM) with tetrabutylammonium bromide (TBAB) at different concentrations in $CDCl_3$ (400 MHz, 298 K). (b) The corresponding binding constant K_{Br^-} were determined by fitting the NMR titration data to a 1:1 binding model using the online fitting tool Bindfit (http://app.supramolecular.org/bindfit/).

^{1}H NMR experiments for amino acids in the presence of 200 equiv. TBAB

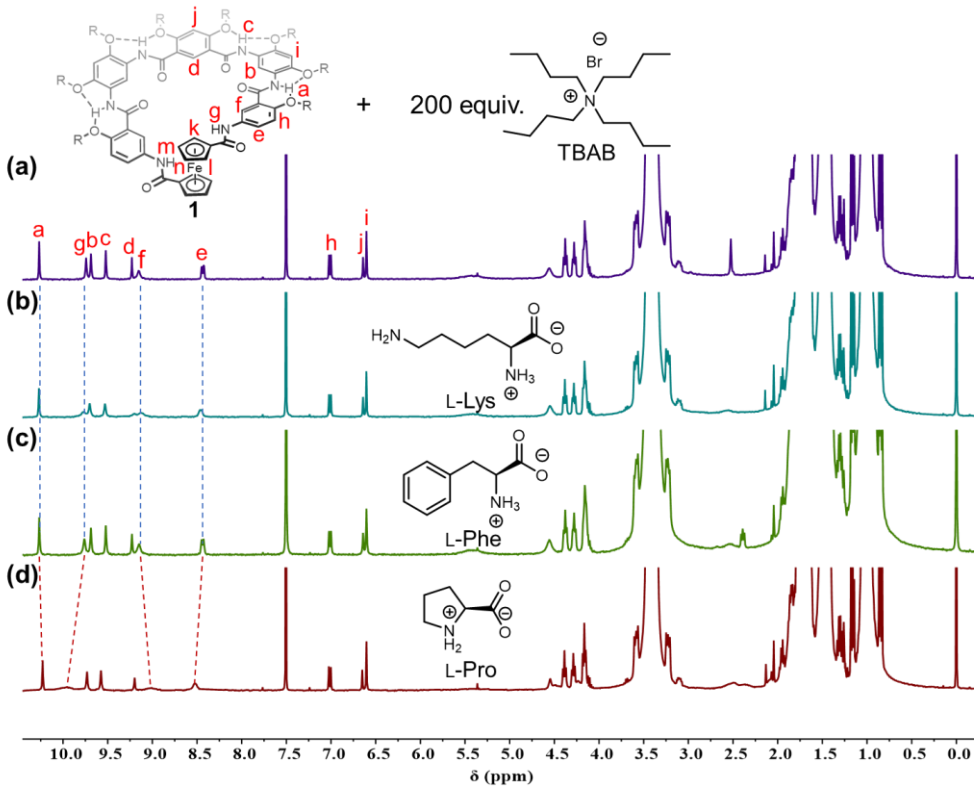

Figure S19 Excerpts of the 400 MHz ^{1}H NMR spectra of 2.0 mM $CDCl_3$ solution of (a) macrocycle **1** in the presence of 200 equiv. TBAB; (b) 1:2.1 mixture of macrocycle **1** and L-lysine in the presence of 200 equiv. TBAB; (c) 1:2.1 mixture of macrocycle **1** and L-phenylalanine in the presence of 200 equiv. TBAB; (d) 1:2.1 mixture of macrocycle **1** and L-proline in the presence of 200 equiv. TBAB.

NMR titration experiments for L-proline in the presence of 200 equiv. TBAB

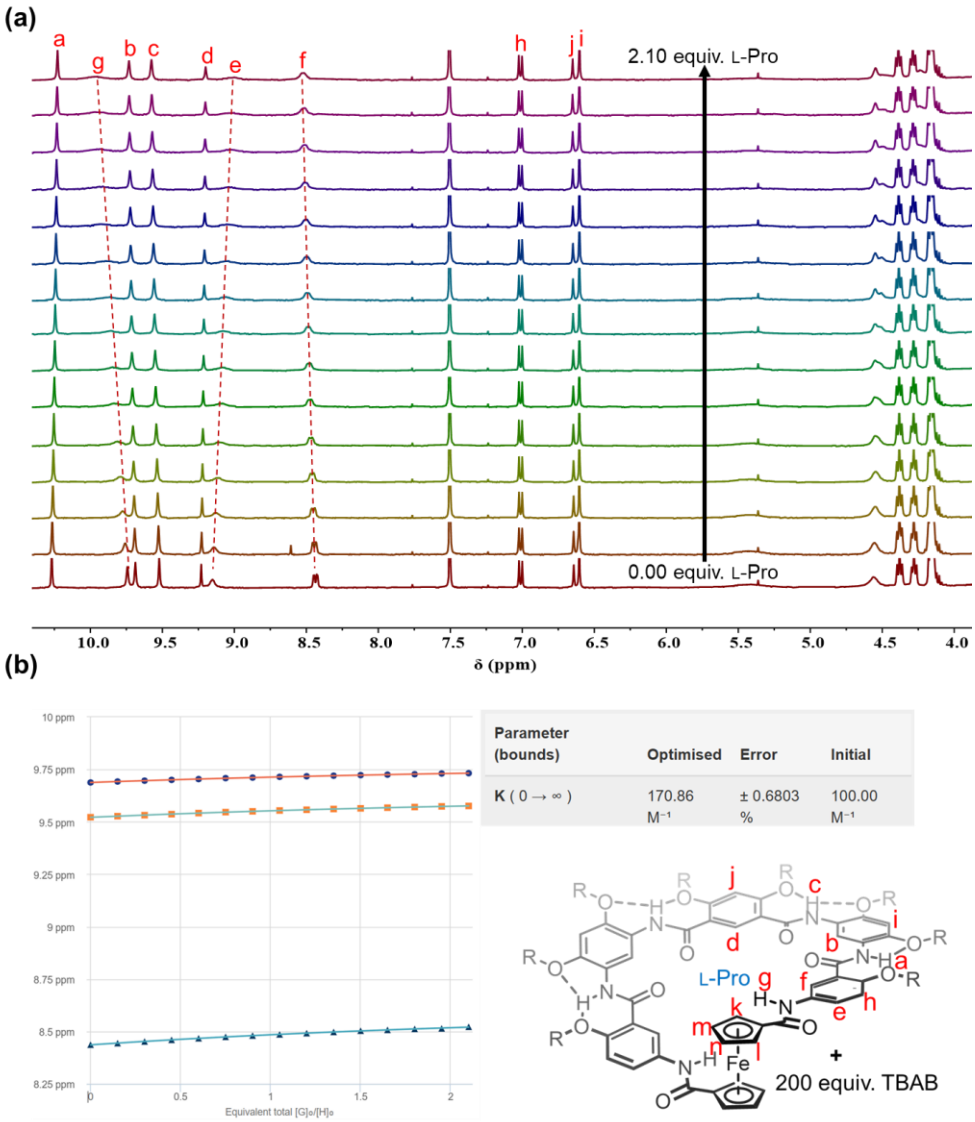

$$K_{\text{rel-L-Pro}} = (1.70 \pm 0.01) \times 10^2\ \text{M}^{-1}$$

$$K_{\text{L-Pro}} = K_{\text{rel}} \times K_{\text{Br}^-} \times [\text{Br}^-] = (1.77 \pm 0.24) \times 10^6\ \text{M}^{-1}$$

Figure S20 (a) Stacked plots of ^{1}H NMR spectra of macrocycle **1** (2.0 mM) with L-Pro at different concentration in the presence of 200 equiv. TBAB in $CDCl_3$ (400MHz, 298K). (b) The corresponding binding constant $K_{\text{rel-L-Pro}}$ were determined by fitting the NMR titration data to a 1:1 binding model using the online fitting tool Bindfit (http://app.supramolecular.org/bindfit/). The $K_{\text{L-Pro}}$ is calculated via the equation listed above while the deviation (ε) of $K_{\text{L-Pro}}$ is estimated via the equation $\varepsilon = 1.77 \times \sqrt{(13.3464\%)^2 \times (0.6803\%)^2} = 0.24$.

9. Host guest complexation between macrocycle 1 and D/L-Pro

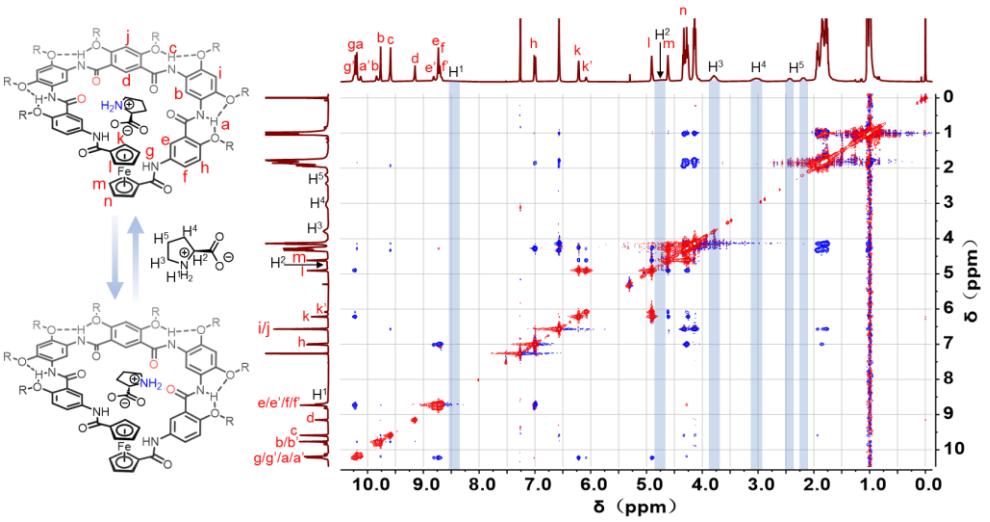

Figure S21 2D ROESY NMR of spectrum of complex L-Pro⊂**1** (400 MHz, [**1**] **=** 10.0 mM, [L-Pro] = 12.0 mM, 298 K, $CDCl_3$).

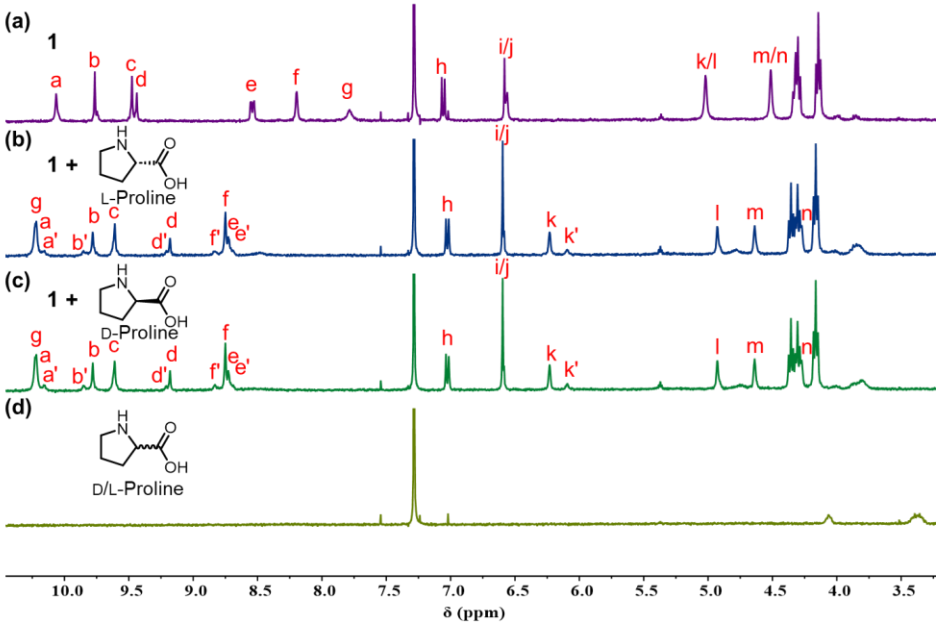

Figure S22 Partially stacked ^{1}H NMR spectra of (a) macrocycle **1**; (b) 1:1 mixture of macrocycle **1** and L-proline; (c) 1:1 mixture of macrocycle **1** and D-proline; (d) D/L-Proline. (400 MHz, 1.0 mM, 298 K, $CDCl_3$).

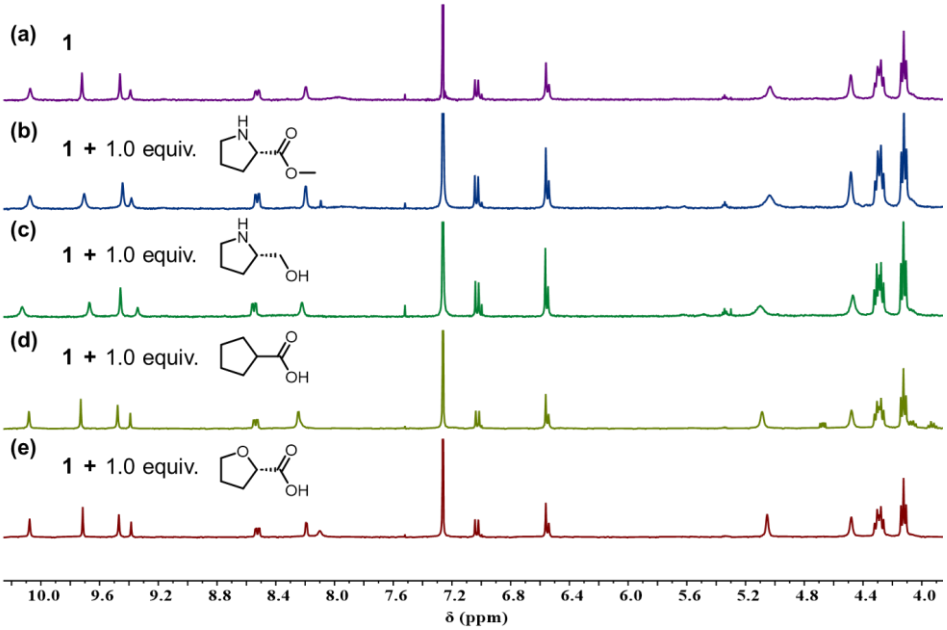

Figure S23 Excerpts of the 400 MHz ^{1}H NMR spectra of 1.0 mM $CDCl_3$ solution of (a) macrocycle **1**, (b) 1:1 mixture of macrocycle **1** and L-proline-OMe, (c) 1:1 mixture of macrocycle **1** and L-prolinol, (d) 1:1 mixture of macrocycle **1** and cyclopentanecarboxylic acid, (e) 1:1 mixture of macrocycle **1** and (*S*)-tetrahydro-2-furoicacid at 298 K.

10. X-ray single crystal structures of 1, Pro⊂1 and 1-Me

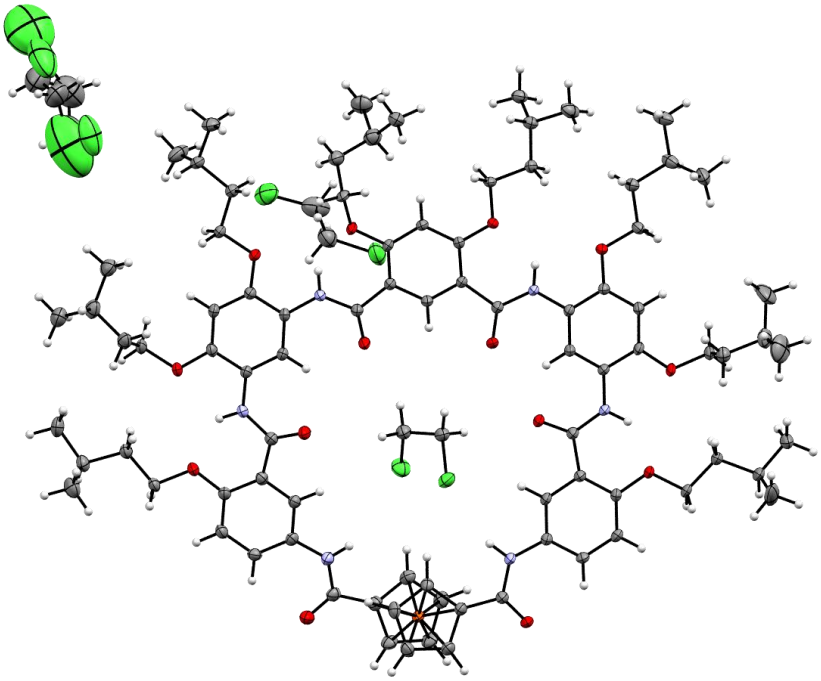

Figure S24 The ORTEP plot of the crystal structures of macrocycle **1**. The thermal ellipsoids are scaled to 50% probability level.

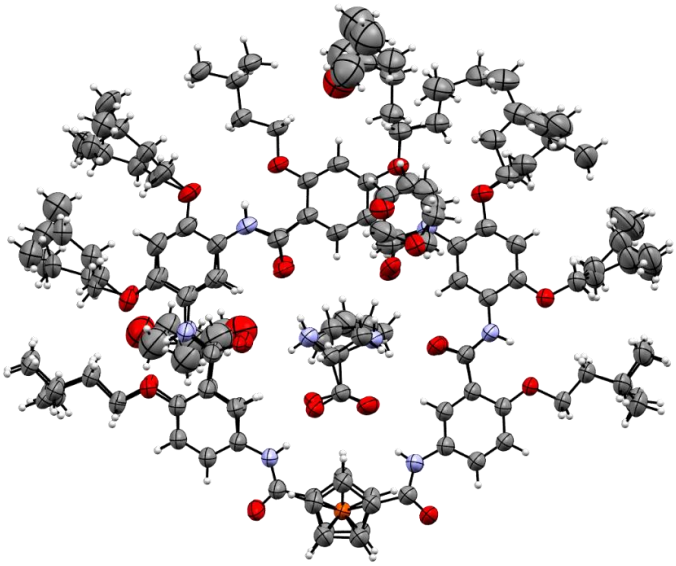

Figure S25 The ORTEP plot of the crystal structures of complex Pro⊂**1**. The thermal ellipsoids are scaled to 50% probability level.

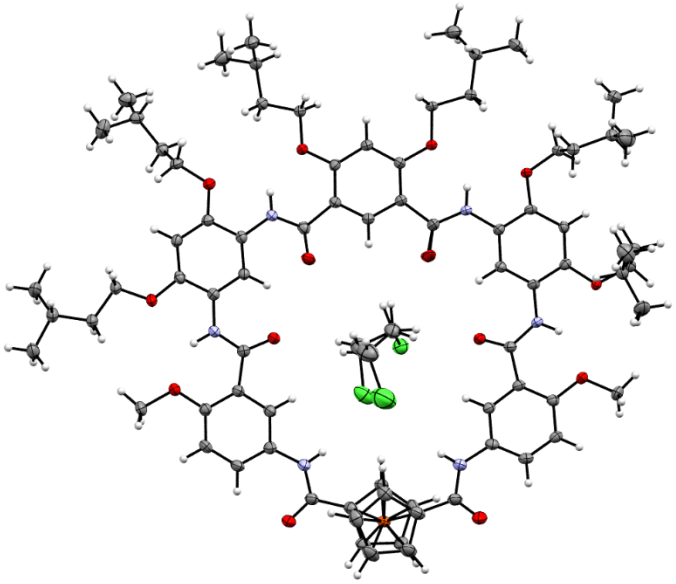

Figure S26 The ORTEP plots of the crystal structures of macrocycle **1-Me**$_{in}$ in the NH inward pointing conformation. The thermal ellipsoids are scaled to 50% probability level.

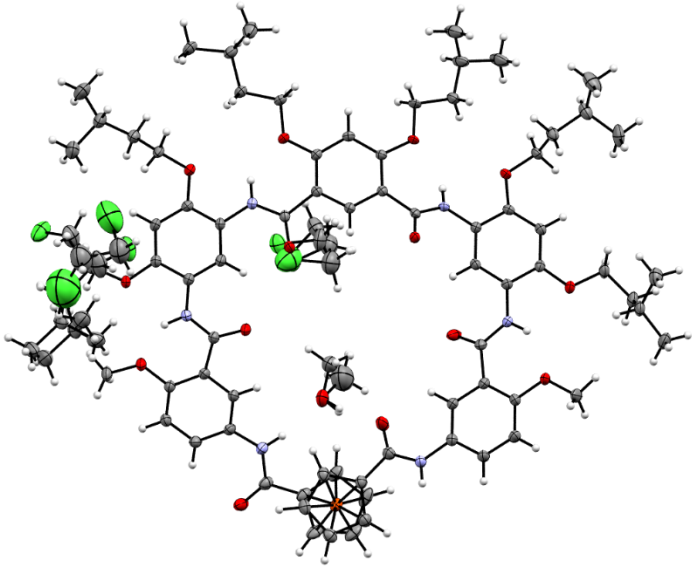

Figure S27 The ORTEP plots of the crystal structures of macrocycle **1-Me**$_{out}$ in the NH outward pointing conformation. The thermal ellipsoids are scaled to 50% probability level.

Table S1 Crystal data and structure refinements for compounds **1**, Pro⊂**1**, **1-Me**$_{in}$ and **1-Me**$_{out}$

Compound	**1**	Pro⊂**1**	**1-Me**$_{in}$	**1-Me**$_{out}$
CCDC number	2497426	2497429	2497427	2497428
Empirical formula	$C_{92}H_{126}Cl_6FeN_6O_{14}$	$C_{202}H_{286}Fe_2N_{14}O_{37}$	$C_{80}H_{102}Cl_2FeN_6O_{14}$	$C_{83}H_{110}Cl_4FeN_6O_{15}$
Formula weight	1808.53	3614.13	1498.42	1629.41
Temperature/K	100.00(10)	100.00(10)	100.01(10)	99.99(16)
Crystal system	triclinic	triclinic	triclinic	monoclinic
Space group	P-1	P-1	P-1	$P2_1/c$
a/Å	15.5789(4)	14.8979(2)	11.7543(2)	18.30930(10)
b/Å	17.0278(3)	18.2361(3)	17.4281(3)	28.5619(2)
c/Å	20.3061(3)	19.1025(3)	19.0083(3)	15.91770(10)
α/°	71.181(2)	96.453(2)	84.0200(10)	90

β/°	78.454(2)	92.8760(10)	88.7430(10)	107.4320(10)
γ/°	64.648(2)	108.818(2)	77.9620(10)	90
Volume/Å^3	4595.56(18)	4860.58(14)	3787.59(11)	7941.83(10)
Z	2	1	2	4
ρ_{calc}g/cm^3	1.307	1.235	1.314	1.363
μ/mm^{-1}	0.403	1.811	0.338	3.329
F(000)	1920.0	1944.0	1592.0	3456.0
Crystal size/mm^3	0.18 × 0.15 × 0.13	0.18 × 0.16 × 0.13	0.15 × 0.13 × 0.12	0.15 × 0.13 × 0.12
Radiation	Mo Kα (λ = 0.71073)	Cu Kα (λ = 1.54184)	Mo Kα (λ = 0.71073)	Cu Kα (λ = 1.54184)
2Θ range for data collection/°	2.99 to 58.64	4.676 to 152.688	3.058 to 58.808	5.058 to 151.92
Index ranges	-21 ≤ h ≤ 20, -21 ≤ k ≤ 22, -23 ≤ l ≤ 27	-18 ≤ h ≤ 18, -20 ≤ k ≤ 22, -24 ≤ l ≤ 23	-14 ≤ h ≤ 15, -18 ≤ k ≤ 23, -24 ≤ l ≤ 25	-23 ≤ h ≤ 23, -30 ≤ k ≤ 35, -19 ≤ l ≤ 13
Reflections collected	65994	60400	44160	56948
Independent reflections	20779 [R_{int} = 0.0356, R_{sigma} = 0.0471]	19708 [R_{int} = 0.0285, R_{sigma} = 0.0313]	16854 [R_{int} = 0.0272, R_{sigma} = 0.0406]	16185 [R_{int} = 0.0330, R_{sigma} = 0.0315]
Data/restraints/parameters	20779/167/1125	19708/2998/1812	16854/71/971	16185/371/1096
Goodness-of-fit on F^2	1.078	1.058	1.060	1.030
Final R indexes [I>=2σ (I)]	R_1 = 0.0574, wR_2 = 0.1555	R_1 = 0.0834, wR_2 = 0.2568	R_1 = 0.0488, wR_2 = 0.1303	R_1 = 0.0662, wR_2 = 0.1930
Final R indexes [all data]	R_1 = 0.0799, wR_2 = 0.1684	R_1 = 0.1066, wR_2 = 0.2881	R_1 = 0.0682, wR_2 = 0.1408	R_1 = 0.0726, wR_2 = 0.1977
Largest diff. peak/hole / e Å^{-3}	1.13/-0.88	0.90/-0.38	0.56/-0.57	0.88/-1.49

Table S2. Cartesian coordinates for the optimized geometry structure of macrocycle **1** and complex glycine⊂**1** (DFT-D3, B3LYP/6-311G(d))

Macrocycle **1** (side chains are omitted as methyl group)

C	-4.37191300	3.15725400	-0.52123800
C	-3.04227300	3.49193600	-0.75879200
C	-2.51220400	4.76557500	-0.58379200
C	-3.39686400	5.78009700	-0.17961900
C	-4.74874300	5.49676300	0.03233300

C	-5.23392800	4.19550300	-0.12564800
H	-2.37309000	2.70416100	-1.07601600
H	-5.42148600	6.28716900	0.32533600
C	-1.02385400	4.86290800	-0.80894500
C	1.00043600	6.11894900	-0.12848100
C	1.92427200	5.08974900	-0.31689600
C	1.45222300	7.37699500	0.29891800
C	3.28193900	5.29101100	-0.06874400
H	1.58677700	4.12747000	-0.65478300
C	2.80944000	7.59525600	0.53227300
C	3.72215100	6.55850300	0.34976800
H	3.15234600	8.56512300	0.85859000
C	-4.68498100	1.68966200	-0.67243600
C	-6.29775800	-0.09023000	-0.11420400
C	-5.39048300	-1.14448300	-0.02819900
C	-7.67250400	-0.36406700	-0.06760400
C	-5.82768600	-2.46177900	0.08340600
H	-4.33659000	-0.93975300	-0.05318200
C	-8.12445100	-1.68052400	0.02990500
C	-7.20603600	-2.72792100	0.09581000
H	-9.18326100	-1.88804100	0.05315400
C	4.05716600	2.97283400	-0.49269800
C	-3.63901300	-3.52283000	0.51925900
C	5.26291400	2.05922300	-0.43533100
C	6.58133600	2.38632900	-0.05830400
C	4.98746000	0.73470500	-0.76328300
C	7.55266700	1.38619900	-0.01457200
C	5.95440700	-0.26775700	-0.72935500
H	3.96220200	0.51338200	-1.03960200
C	7.25468100	0.06665300	-0.34415000
H	8.56728600	1.62185800	0.27804000
H	8.01623000	-0.69638100	-0.30057500
C	-2.86029900	-4.81686600	0.42913600
C	-3.32972500	-6.08252100	0.02185100
C	-1.51423200	-4.69528500	0.76250500

C	-2.44100500	-7.15533500	-0.04712800
C	-0.62310000	-5.76472300	0.70312500
H	-1.18359100	-3.70721400	1.06397100
H	-2.78498300	-8.13125700	-0.36265300
C	6.22664100	-2.74929000	-0.93974200
C	4.27807100	-6.47476400	1.58999900
C	3.41214200	-4.33070300	1.58779900
C	5.32790100	-5.57335300	1.90959900
H	4.34311300	-7.54565300	1.47926300
C	4.79605300	-4.25123700	1.90610100
H	2.75458300	-3.48099400	1.47038200
H	6.36177400	-5.83470300	2.07776100
H	5.35976500	-3.34267400	2.06021400
C	6.02859000	-5.26541300	-1.32567200
C	4.05885600	-4.09863400	-1.64771100
C	5.00714300	-6.20013100	-1.63982900
H	7.05939300	-5.47458600	-1.08753600
C	3.79242000	-5.48224300	-1.83789200
H	3.31524700	-3.31630500	-1.70375300
H	5.11573200	-7.27363500	-1.67535800
H	2.82572200	-5.92078900	-2.03744300
O	-0.43981200	3.95391900	-1.37454600
O	-3.84478300	0.93886200	-1.14092100
O	-3.07309400	-2.50437100	0.89050600
O	2.96781000	2.50576800	-0.79158400
O	7.36978500	-2.82856300	-0.51397900
H	-0.96116800	6.70671600	0.07194000
H	-6.58723400	1.95062300	0.03570300
H	5.20253200	4.56673100	0.04995600
H	4.61661600	-1.62479300	-1.47415500
H	0.87537700	-4.60137600	1.47362100
H	-5.35400900	-4.46653900	-0.05136800
N	-0.38657400	5.95347200	-0.27624500
N	-4.95293300	-3.56090000	0.14653400
N	5.54675100	-1.56706500	-1.09128600

N	0.71310100	-5.51145800	1.07248700
N	-5.89664500	1.25444600	-0.20151100
C	5.45335800	-3.95603600	-1.32926000
C	3.08222900	-5.71554800	1.39162500
Fe	4.51853000	-5.12921800	0.06009000
O	-6.54538300	3.88254500	0.08902100
O	-2.88208800	7.03331600	-0.01352100
O	-8.49821700	0.73294300	-0.11499700
O	-7.55326400	-4.05433000	0.16940500
O	0.47650000	8.32901800	0.48066400
O	5.07469900	6.67755200	0.56384100
O	6.84883600	3.69384400	0.25448100
O	-4.65892300	-6.20042100	-0.29126400
N	4.25998300	4.28907500	-0.18671100
C	-8.92718100	-4.38835900	0.17147700
H	-9.44232300	-3.95763200	1.03718100
H	-9.42246000	-4.05556900	-0.74754400
H	-8.97331500	-5.47417900	0.23287100
C	-9.89534900	0.52069100	-0.06998200
H	-10.23646000	-0.08096500	-0.91961600
H	-10.19799600	0.03346600	0.86373900
H	-10.35257600	1.50713500	-0.12531600
C	-7.45501000	4.88978200	0.50191800
H	-7.15666600	5.32653500	1.45981500
H	-7.54252700	5.67693700	-0.25296300
H	-8.41383600	4.38868500	0.61493000
C	-3.72759300	8.09571900	0.39717100
H	-4.52087200	8.27475300	-0.33468100
H	-4.16768600	7.89739000	1.37932300
H	-3.08651100	8.97244200	0.45652800
C	-5.16304000	-7.45173700	-0.72854800
H	-4.66829300	-7.77930900	-1.64775400
H	-5.04793200	-8.21817000	0.04391400
H	-6.22087500	-7.28844500	-0.92384700
C	0.86455500	9.60373900	0.95210500

H	1.34071500	9.53991200	1.93695700
H	1.54541200	10.10001100	0.25179400
H	-0.05071200	10.18775200	1.03337700
C	5.58122400	7.93037600	0.97790600
H	5.37966700	8.70956800	0.23456900
H	5.16202200	8.23338400	1.94389600
H	6.65766400	7.80292100	1.07918700
C	8.15841500	4.06085700	0.65415800
H	8.45768300	3.53407900	1.56537200
H	8.88551600	3.86378000	-0.13943900
H	8.11470600	5.13014100	0.85012900
C	1.80312100	-6.33726700	0.96317800
O	1.75149900	-7.48794800	0.55303300
C	-1.09697700	-7.01057900	0.28602400
H	-0.42136600	-7.84949600	0.22401000

Complex glycine⊂**1** (side chains are omitted as methyl group)

C	5.40560600	1.15413100	0.81110900
C	4.27060000	1.94808800	0.82888900
C	4.24133900	3.29414900	0.48496700
C	5.47316200	3.89436800	0.15727000
C	6.64844600	3.13761300	0.15731600
C	6.61773100	1.77213100	0.46101800
H	3.34387300	1.46819300	1.10111000
H	7.58652300	3.60938600	-0.08937300
C	2.86819500	3.89180100	0.42878900
C	1.58012900	5.92816000	-0.15033700
C	0.31471900	5.35959700	-0.07670800
C	1.69756400	7.28334700	-0.49850700
C	-0.83353700	6.09221800	-0.35469500
H	0.22895600	4.32929800	0.19210000
C	0.55335000	8.03929000	-0.75554800

C	-0.71134800	7.44997500	-0.68580000
H	0.64525900	9.08278500	-1.01518200
C	5.12844700	-0.30231800	1.08159200
C	5.80841100	-2.57687100	0.43672900
C	4.52064700	-3.09434500	0.30628200
C	6.91332300	-3.42206800	0.28709500
C	4.31204100	-4.44101500	0.02946300
H	3.66824300	-2.45233100	0.42183400
C	6.72070200	-4.78018800	0.02658500
C	5.42924000	-5.28915800	-0.09609700
H	7.57074600	-5.43639600	-0.08255100
C	-2.42473500	4.21237600	-0.22243000
C	1.84219200	-4.37023600	-0.24773200
C	-3.82563200	3.82213900	0.11456700
C	-4.94761100	4.67436200	0.18316800
C	-3.99403200	2.47656700	0.43139800
C	-6.17740200	4.14488300	0.56394900
C	-5.21688900	1.94094200	0.83540500
H	-3.13757600	1.82161100	0.37811200
C	-6.32318600	2.79805300	0.89329300
H	-7.05325200	4.77799900	0.61664800
H	-7.28274700	2.40894400	1.19471700
C	0.63272900	-5.24272500	-0.46914400
C	0.59134700	-6.65449600	-0.45868300
C	-0.55440700	-4.55054500	-0.70505300
C	-0.61782600	-7.30551500	-0.68147900
C	-1.77376900	-5.19842200	-0.92311200
H	-0.51473200	-3.46950500	-0.72182600
H	-0.66696100	-8.38641500	-0.67812200
C	-6.32984800	-0.17094800	1.50816900
C	-6.60564100	-4.04876700	-1.46176700
C	-5.05367000	-2.33276000	-1.57118400
C	-7.31231600	-2.81784500	-1.48779700
H	-7.01807900	-5.04209700	-1.38358000
C	-6.35587800	-1.76164200	-1.55706100

H	-4.11963800	-1.79120200	-1.56990700
H	-8.38339200	-2.69691600	-1.42036300
H	-6.57904400	-0.70452900	-1.54132000
C	-7.11682300	-2.56742200	1.85806600
C	-4.81649400	-2.32833100	1.68597300
C	-6.53396100	-3.86118600	1.89710600
H	-8.16579500	-2.31830300	1.88321500
C	-5.11886400	-3.71300500	1.79205100
H	-3.83289000	-1.90231500	1.55124600
H	-7.06863500	-4.79809000	1.94882600
H	-4.39987800	-4.51771700	1.74103900
O	1.88920700	3.17801900	0.66952700
O	4.06030000	-0.62120400	1.58326000
O	1.72801900	-3.15060900	-0.19097300
O	-1.56348900	3.34318900	-0.40703500
O	-7.46083900	0.28937600	1.61036800
H	3.62624700	5.70699900	-0.07261800
H	6.96038400	-0.85838500	0.36638900
H	-2.89907600	6.18731400	-0.21797400
H	-4.32815000	0.11296500	1.07932300
H	-2.74637500	-3.39494600	-1.02295100
H	3.03014800	-6.02434500	-0.21703800
N	2.76370300	5.20353100	0.08375800
N	3.04652600	-5.01662900	-0.13429600
N	-5.23224300	0.57870900	1.15702800
N	-2.90679400	-4.39557800	-1.13228100
N	6.04839500	-1.20194200	0.62817100
C	-6.06060700	-1.61038800	1.72486300
C	-5.20547800	-3.75869700	-1.50616600
Fe	-6.03482600	-2.88740000	0.13907700
O	7.73068800	0.99063800	0.43963900
O	5.46476200	5.22036200	-0.15745600
O	8.14423900	-2.81848000	0.38858600
O	5.14318800	-6.60693400	-0.34398000
O	2.97760400	7.77098800	-0.56364700

O	-1.88634700	8.11432700	-0.90661100
O	-4.76498200	5.99820300	-0.14020000
O	1.76271100	-7.33753900	-0.22330600
N	-2.12240400	5.53932800	-0.25849000
C	6.21707100	-7.51408900	-0.49620200
H	6.85623100	-7.23862300	-1.34225500
H	6.82384300	-7.57302300	0.41414700
H	5.76535900	-8.48501500	-0.69071400
C	9.29655900	-3.62431000	0.23569100
H	9.34051200	-4.40781500	0.99988200
H	9.33652000	-4.08450400	-0.75792500
H	10.14916500	-2.95854100	0.35825900
C	8.98425000	1.55476200	0.07887100
H	8.95845800	1.95944700	-0.93714300
H	9.28121900	2.33621100	0.78409400
H	9.69705400	0.73504500	0.12599600
C	6.66835500	5.86788500	-0.54650900
H	7.40122000	5.85790800	0.26516900
H	7.09461400	5.40323100	-1.43999900
H	6.38704700	6.89435700	-0.76933400
C	1.74694400	-8.75280100	-0.18813500
H	1.08603200	-9.12289400	0.60154100
H	1.43721200	-9.17289900	-1.15024600
H	2.77121700	-9.05158300	0.02720000
C	3.16174700	9.13185000	-0.91096300
H	2.77148600	9.34402800	-1.91184300
H	2.68365600	9.79644100	-0.18390200
H	4.23646900	9.30293400	-0.89981600
C	-1.83424000	9.49473200	-1.21980000
H	-1.37605100	10.07084300	-0.40876000
H	-1.28455400	9.67158900	-2.15023700
H	-2.86696500	9.81203900	-1.34854900
C	-5.87795900	6.87666700	-0.09616400
H	-6.65688400	6.56140200	-0.79643400
H	-6.29578700	6.93883000	0.91318600

H	-5.49554800	7.85140900	-0.39258100
C	-4.18418900	-4.82863300	-1.37969500
O	-4.50689900	-6.00833900	-1.46796300
C	-1.79341600	-6.59750300	-0.91205500
H	-2.72111400	-7.11898500	-1.08369900
C	-0.29346500	-0.10134200	-0.29039900
H	-0.16281800	0.15643200	-1.33919900
C	-1.69459800	-0.72311100	-0.05259100
O	-2.35197300	-0.21821200	0.89605600
O	-1.99520400	-1.64986800	-0.82168700
H	-0.73706700	1.91506600	0.13140300
N	-0.17025700	1.14606800	0.53285800
H	0.78044600	1.51327900	0.64628800
H	0.48510600	-0.80886000	-0.00045600
H	-0.60324000	0.94048200	1.43713900

References

1. Becke, A. D., Density‐functional thermochemistry. III. The role of exact exchange. *J. Chem. Phys.*, **1993**, *98*, 5648-5652.
2. Grimme, S.; Antony, J.; Ehrlich, S.; Krieg, H., A consistent and accurate ab initio parametrization of density functional dispersion correction (DFT-D) for the 94 elements H-Pu. *J. Chem. Phys.*, **2010,** *132*, 154104.
3. Frisch, M. J.; Trucks, G. W.; Schlegel, H. B.; Scuseria, G. E.; Robb, M. A.; Cheeseman, J. R.; Scalmani, G.; Barone, V.; Mennucci, B.; Petersson, G. A.; Nakatsuji, H.; Caricato, M.; Li, X.; Hratchian, H. P.; Izmaylov, A. F.; Bloino, J.; Zheng, G.; Sonnenberg, J. L.; Hada, M.; Ehara, M.; Toyota, K.; Fukuda, R.; Hasegawa, J.; Ishida, M.; Nakajima, T.; Honda, Y.; Kitao, O.; Nakai, H.; Vreven, T.; Montgomery, J. A., Jr; Peralta, J. E.; Ogliaro, F.; Bearpark, M.; Heyd, J. J.; Brothers, E.; Kudin, K. N.; Staroverov, V. N.; Kobayashi, R.; Normand, J.; Raghavachari, K.; Rendell, A.; Burant, J. C.; Iyengar, S. S.; Tomasi, J.; Cossi, M.; Rega, N.; Millam, J. M.; Klene, M.; Knox, J. E.; Cross, J. B.; Bakken, V.; Adamo,

C.; Jaramillo, J.; Gomperts, R.; Stratmann, R. E.; Yazyev, O.; Austin, A. J.; Cammi, R.; Pomelli, C.; Ochterski, J. W.; Martin, R. L.; Morokuma, K.; Zakrzewski, V. G.; Voth, G. A.; Salvador, P.; Dannenberg, J. J.; Dapprich, S.; Daniels, A. D.; Farkas, Ö .; Foresman, J. B.; Ortiz, J. V.; Cioslowski, J.; Fox, D. J. Gaussian 09, Revision E. 01; Gaussian Inc.: Wallingford CT, 2013.

4. (a) Petersson, G. A.; Bennett, A.; Tensfeldt, T. G.; Al-Laham, M. A.; Shirley, W. A.; Mantzaris, J., A complete basis set model chemistry. I. The total energies of closed-shell atoms and hydrides of the first-row elements. *J. Chem. Phys.*, **1988,** *89*, 2193-2218. (b) Petersson, G. A.; Al-Laham, M. A., A complete basis set model chemistry. II. Open-shell systems and the total energies of the first-row atoms. *J. Chem. Phys.*, **1991,** *94*, 6081-6090.
5. (a) Li, X. H.; Fang, Y. Y.; Deng, P. C.; Hu, J. C.; Li, T.; Feng, W.; Yuan, L. H., Self-Complementary Quadruply Hydrogen-Bonded Duplexes Based on Imide and Urea Units. *Org. Lett.*, **2011,** *13*, 4628-4631. (b) Zhang, Y. K.; Cao, R. K.; Shen, J.; Detchou, C. S. F.; Zhong, Y. L.; Wang, H.; Zou, S.; Huang, Q. F.; Lian, C. X.; Wang, Q. W.; Zhu, J.; Gong, B., Hydrogen-Bonded Duplexes with Lengthened Linkers. *Organic Letters*, **2018,** *20*, 1555-1558. (c) Huang, S. Q.; Yang, R.; Wang, J. D.; Chang, S. A.; Gou, X. F.; Hua, C. W.; Zhao, J. L., Synthesis and combustion catalytic activity of ferrocene-based energetic compounds. *J. Hetero. Chem.*, **2020,** *57*, 2854-2861.
6. Cao, R. K.; Rossdeutcher, R. B.; Zhong, Y.L.; Shen, Y.; Miller, D. P.; Sobiech, T. A.; Wu, X. X.; Buitrago, L. S.; Ramcharan, K.; Gutay, M. I.; Figueira, M. F.; Luthra, P.; Zurek, E.; Szyperski, T.; Button, B.; Shao, Z. F.; Gong, B., Aromatic pentaamide macrocycles bind anions with high affinity for transport across biomembranes. *Nat. Chem.*, **2023,** *15*, 1559-1568.